neuroglia

MDPI

Article

Investigating Glial Fibrillary Acidic Protein Expression and Cell Morphology in a Rat Brain Following Exposure to a Weak Electromagnetic Field and Nitric Oxide Modulation During Development

Stephanie M. Sissons [1,2,3], Nirosha J. Murugan [2,4] and Blake T. Dotta [1,2,*]

[1] Behavioural Neuroscience, Laurentian University, Sudbury, ON P3E2C6, Canada; ssissons@trentu.ca
[2] Biology Programs, Laurentian University, Sudbury, ON P3E2C6, Canada; nmurugan@wlu.ca
[3] Psychology Program, Trent University, Peterborough, ON K9L0G2, Canada
[4] Department of Health Sciences, Wilfred Laurier University, Waterloo, ON N2L3C5, Canada
* Correspondence: bx_dotta@laurentian.ca; Tel.: +1-705-675-4824

Abstract: Background/Objectives: Nitric oxide (NO) and electromagnetic fields (EMFs) have been reported to influence central nervous system (CNS) function and organization. This study explores the effects of NO modulation and EMF exposure on neurodevelopment and glial fibrillary acidic protein (GFAP) expression and cell morphology, extending the prior work on perinatal EMF exposure in Wistar rats. Methods: Rats were perinatally exposed to water, 1 g/L L-arginine (LA), or 0.5 g/L N-methylarginine (NMA), along with a 7 Hz square-wave EMF at intensities of 0 nT, ≤50 nT, or 500 nT, starting three days before birth and continuing for 14 days postnatally. GFAP expression and cell morphology were analyzed via immunohistochemistry in regions including the hypothalamus, amygdala, hippocampus, and cortex. Results: Significant changes in GFAP morphology and expression are observed. A main EMF effect emerged in the right ventromedial hypothalamus, where the branch length of GFAP-expressing cells increased in EMF-exposed groups compared to the controls [$t(32) = -2.52$, $p = 0.017$]. In the hippocampus, LA exposure decreased GFAP expression in the right dentate gyrus compared to water controls [$t(23) = 2.37$, $p = 0.027$]. A sex-specific EMF effect was detected in the left CA2 hippocampus, where males exposed to EMF showed significant differences from unexposed males [$t(15) = -2.90$, $p = 0.011$]. Conclusions: These findings reveal complex interactions between EMF exposure, sex, and NO modulation, with region-specific effects on GFAP expression in the developing rat brain.

Keywords: neurodevelopment; nitric oxide; electromagnetic fields; GFAP expression; rat brain

check for updates

Academic Editor: Jessica Filosa

Received: 29 January 2025
Revised: 17 April 2025
Accepted: 22 April 2025
Published: 3 May 2025

Citation: Sissons, S.M.; Murugan, N.J.; Dotta, B.T. Investigating Glial Fibrillary Acidic Protein Expression and Cell Morphology in a Rat Brain Following Exposure to a Weak Electromagnetic Field and Nitric Oxide Modulation During Development. *Neuroglia* **2025**, *6*, 21. https://doi.org/10.3390/neuroglia6020021

Copyright: © 2025 by the authors. Licensee MDPI, Basel, Switzerland. This article is an open access article distributed under the terms and conditions of the Creative Commons Attribution (CC BY) license (https://creativecommons.org/licenses/by/4.0/).

1. Introduction

Neurons, astrocytes, and microglia communicate with one another in the central nervous system (CNS) [1,2]. The accuracy and speed of this communication, which depend on the complementary functions of diverse cell types, are crucial for modulating neurodevelopment and overall brain functioning as well as maintaining homeostasis, especially during inflammatory states and microenvironmental changes [1,2]. In particular, glial cells maintain brain homeostasis by regulating oxidative stress; buffering excitotoxic ions, such as calcium; recycling metabolites; clearing dead cells; absorbing toxins; regulating water; and buffering pH [1]. As one of the most-abundant and diverse cells in the CNS,

astroglia provide functional and structural support for blood vessels and neurons; maintain and regulate cytoarchitecture, metabolism, synaptic transmission, and inflammation processes; and modulate neurotransmitters [1–4]. Glial cells in general play important roles in the maintenance of the structure and function of the CNS and the BBB, along with the modulation of nutrient uptake in accordance with the brain's needs [2,4].

The glial fibrillary protein (GFAP) is a common astrocytic cytoskeleton intermediate filament protein, which is expressed by most activated astrocytes within the CNS, making it an ideal marker of astrogliosis [1,4–7]. Additionally, the GFAP is implicated in many beneficial physiological and pathophysiological functions within the CNS, including the modulation of synaptic efficacy, CNS myelination, BBB integrity, and the shape and movement of astrocytes [4,6–8]. GFAP-expressing astrocytes have also been shown to influence sleep, breathing, learning, memory, and BBB permeability [4,6,7,9]. However, the activation of astrocytes causing alterations in GFAP expression can be either cytoprotective or cytotoxic, depending on their concentration and activation phenotype [1,5–7]. For example, high levels of the GFAP contribute to the promotion of neurotoxicity and inflammation, neuronal dysfunction, apoptosis, and decreased neuronal plasticity, and have been implicated in a wide variety of neurodegenerative and inflammatory conditions, like Alzheimer's and Parkinson's disease [5–8,10].

Nitric oxide (NO) can be derived from activated glial cells and is a modulator of many processes, including cell proliferation, apoptosis, angiogenesis, degeneration of myelin, cancer, and, depending on its concentration, the progression of neurodegenerative disease [2,8]. NO is important in the facilitation of neuron-glial interactions and the regulation of astrocyte activation and expression of GFAP [7]. Studies report that increases in NOS facilitated by microglia can lead to neuronal damage and or death through NO-dependent microglia cell-mediated cytotoxicity [2,7]. Additionally, the NO/guanylate cyclase/cGMP pathway along with general increases in NO have been shown to regulate the GFAP expression in astrocytes [8]. GFAP, nestin, vimentin, and iNOS are all proteins which have increased expression following CNS injury, neurotoxicity, and inflammatory or ischemic damage [2,8]. In healthy brains, however, neither astroglia nor microglia express iNOS, and in cases where NO and iNOS are depleted, a strong decrease in GFAP expression is noted [2,11].

Sexual dimorphism exists in many areas of the brain, including in the expression of the GFAP and the number, morphology, and maturation of astrocytes present within the CNS [12]. In general, females have more microglia and higher GFAP expression than males in adulthood, however the inverse is true during early postnatal stages [3,4]. This could be explained by sex-dependent hormone profiles causing changes in the function, morphology, and protein expression of cortical astroglia [3]. In particular, estradiol is suggested to mediate the sprouting of neurons and regulate the expression of the GFAP, through its influence on astrocytes [12]. These hormone-mediated effects on astrocytes are known to be region-specific and developmentally dynamic. For instance, estradiol has been shown to upregulate GFAP expression in the arcuate nucleus but suppress it in other hypothalamic regions, suggesting context-dependent astrocyte reactivity [4,12,13]. Additionally, sex differences in glial activation and morphology have been observed in response to injury, inflammation, and environmental exposures, often linked to circulating levels of estradiol, progesterone, and testosterone [4,12,13]. Based on these findings, we expected sex-dependent differences in GFAP expression and astrocyte morphology in the current study, particularly in response to EMF and nitric oxide modulation during development.

Previous studies have investigated the effect of NO modulation and perinatal electromagnetic field (EMF) exposure on the developing rat brain [14]. It was found that perinatal exposure to a 7 Hz square-wave EMF resulted in long-term behavioral changes

in offspring, including increased movement, rearing, and body weight [14]. Following this, a histological investigation was performed, examining the changes in neuronal counts across a wide variety of brain structures, which have functions correlating with previous behavioral data [15]. It was found that EMF exposure can cause significant alterations in neuronal density, specifically in the secondary somatosensory cortex, hippocampus of female rats only, and entorhinal cortex of male rats only [15]. Additionally, the modulation of NO resulted in neuronal count changes within the ventromedial hypothalamic nucleus and the amygdala [15].

The present study aims to expand on past work by looking at the changes in GFAP expression in the developing rat brain following NO modulation and EMF exposure, since NO can modulate the GFAP expression in astrocytes, and the expression of GFAP can be reduced with exposure to a pulsed EMF [11,16]. Structures for analysis were chosen based on the results of the previous histological study and include the hippocampus (CA1, CA2, CA3, Dentate gyrus), amygdala, entorhinal cortex, primary and secondary somatosensory cortices, and ventromedial hypothalamus. The integration of behavioral data, neuron counts, and GFAP expression will allow for a more complete picture of exactly how prenatal exposure to EMF and NO modulation affects the structure of the developing brain.

2. Methods

2.1. Materials

Detailed descriptions of materials and methods were previously described by Sissons and Dotta [15]. Briefly, histological slides were created using preserved n = 40 albino Wistar rat brains obtained from the previous experiment completed in 2007 by Whissell and Persinger [14]. During the initial experiment, rats were exposed perinatally, from 2 days before birth to 14 days after birth, to NO modulation through the oral administration of either tap water (H_2O), 1 g/L L-Arginine (LA), or 0.5 g/L N-methylarginine (NMA) (the mothers ingested compounds orally during the before-birth stage and the pups for 14 days after birth; daily fluid consumption measurements showed no differences between the three treatments) and a 7 Hz square-wave electromagnetic field at three separate intensities (5 nT, $\leq$50 nT, and 500 nT). The presence of the EMF and its intensity were verified using an amplifier and a magnetometer, respectively. After the exposure period, animals were housed under standard conditions until adulthood. Brains were harvested at an average age of 568 days (SD = 161), ensuring that all observed effects reflected persistent outcomes of early developmental exposure. The brains of those rats were then preserved in an ethanol–formalin–acetic (EFA) acid fixative and embedded in paraffin. The paraffin-embedding procedure was as follows: rat brains were removed from the EFA fixative and wrapped in gauze, then dehydrated through a series of EtOH baths. The EtOH was then cleared from the tissue using a chloroform bath. Following this, the brains were paraffinized through a series of molten paraffin baths and placed in paraffin cubes. The solidified paraffin cubes were then cut from the anterior commissure to the posterior commissure into 10 micron sections and mounted onto microscope slides.

2.2. Staining

Slides were immunostained for GFAP manually using Abcam's standard mouse Specific HRP/DAB (ABC) Detection IHC Kit (ab64259). The entire staining process was performed at room temperature, and each of the buffer washes was performed in Tris Buffer Saline (TBS) with Tween 20 for five minutes with gentle agitation. Ten unstained slides were first loaded into a slide boat and then placed in a container of 100% Xylene for three minutes, then moved to a fresh container of 100% xylene for three minutes, and finally

they were moved to a 1:1 100% Xylene:100% EtOH solution for three minutes. Xylene was used to deparaffinize the slides. Next, the slides spent three minutes each in a series of EtOH baths (100% EtOH, 100% EtOH, 95% EtOH, and 70% EtOH, 50% EtOH). The EtOH dilutions were used to dehydrate, then slowly rehydrate the tissue. The slides were then rinsed in tap water, removed from the boat, and placed on a paper towel. Then, enough drops of a hydrogen peroxide block to cover the tissue were placed onto the sections and incubated for 10 min. The hydrogen peroxide block was used to block endogenous peroxide activity and reduce nonspecific background staining. Following the hydrogen peroxide block incubation, the slides were washed in buffer, twice. Then, heat-induced epitope retrieval was performed, where the slides were boiled in a sodium citrate buffer for 20 min, then cooled in running tap water for 10 min. This retrieval was performed to unmask the target antigen. Following antigen retrieval, a protein block was applied to the tissue and incubated for 10 min at room temperature, then was washed three times in washing buffer. The protein block bound to non-specific sites, thereby reducing non-specific binding. Next, the primary antibody, monoclonal anti-glial fibrillary acidic protein (GFAP) produced in mouse (Sigma-Aldrich G3893, St. Louis, MO, USA) diluted to 1:400 using phosphate buffered saline (PBS) with Tween 20, was applied to the tissue and incubated for two hours at room temperature in a humidified box. Following this, slides were washed four times in washing buffer. Then, the secondary antibody, Biotinylated Goat Anti-Mouse antibody, was applied and incubated at room temperature for 10 min. The slides were then washed four times in washing buffer. Then, streptavidin peroxidase was applied to the slides and incubated at room temperature for 10 min. Slides were then washed an additional four times in washing buffer. Next, one drop of 3,3′-Diaminobenzidine (DAB) chromogen was applied to the slides and incubated in the range of 1–10 min, allowing for the adequate coloring of slides. DAB acts as a substrate for the peroxidase enzymes, to which the secondary antibody is conjugated, producing a brown precipitate that allows for the visualization of the target antibodies. Slides were then rinsed four times in washing buffer. Lastly, a coverslip was applied, and the slides were allowed to dry overnight before imaging. Although negative controls omitting the primary antibody were not included in this study, the GFAP antibody used had a well-established specificity, and the observed staining patterns were consistent with the expected anatomical distribution of astrocytes in the rat brain.

2.3. Data Collection

Imaging, capturing, and quantification were performed by a single observer in a double-blind fashion. Stained sections were viewed using light microscopy (Lumenera Infinity 3 digital Cmos microscope camera) and imaged at 400× magnification using image capture software (infinity capture v4.0.2). The brain regions were located using atlases published by Paxinos and Watson [17]. For each animal and brain region, all GFAP-expressing astrocytes visible within the microscope field at 400× magnification were included in the analysis, consistent with prior cell quantification approaches used in neuron counting studies. The data were averaged at the animal level, with each animal contributing one value per region for statistical analysis. Due to the nature of the stain process, some structures were damaged and could not be imaged; these structures were excluded from the data analysis. Images were then loaded into Fiji (ImageJ) software; the scale was set using the set-scale function and the burned micromotor on the photo. The scale bar was then cropped from the photo. The image was then transformed into an 8 bit image, gray-scaled, and the bandpass filter was applied with a 100 pixel threshold. Then, the unsharp mask filter was used, the photo was despeckled to remove background noise, and the color threshold of the photo was set to max entropy. The photo was then converted

to a binary mask, again background noise was removed using the despeckle function, and outliers (objects less than six pixels) were removed. The particles were then analyzed; this function counted the cells in the photo. Next, the photo was skeletonized to allow for the quantification of the branching of the astrocytes, and the skeleton was analyzed providing outputs for the branch number and length for each cell. Branching was defined by the software as any segment between two junctions (i.e., bifurcations or endpoints) in the skeletonized image. All branches, regardless of order, were included in the analysis, and no distinction was made between primary, secondary, or tertiary protrusions. For each cell, total branch length and number of branches were used to calculate a single mean branch length value. The data were then loaded into Excel and the number of cells, average cell surface area, number of branches, total branch length, and average branch length were computed.

2.4. Data Analysis

All the data were curated and analyzed in SPSS software V28. Initial analysis began with one-way analysis of variances (ANOVAs) to examine the relationships between each of the variables (number of cells, average cell surface area, number of branches, total branch length, and average branch length, compared against drug condition (H_2O, LA, NMA), field exposure (with EMF, without EMF), field exposure intensity (0 nT, $\leq$50 nT, 500 nT), and sex). Following this, independent t-tests were performed to further examine areas of significance. Homogeneity violations were accounted for by using the Kruskal–Willis and Mann–Whitney non-parametric tests. In addition, both Pearson's and Spearman's correlations were reported when examining the quantitative relationships between structures. The paper we submitted did not focus on animal research; it utilized stored tissue. At no point did we handle live animals or require ethics approval. The original study, in which live animals were used, was approved almost 20 years ago by the LU Animal Care Committee. However, since we only used previously collected tissue, no additional ethics approval was required. The Laurentian University Animal Care Committee reviewed and granted permission for this study. Approval code: 980018; approval date: 1 May 2004.

3. Results

3.1. Drug and EMF Main Effects

Upon the completion of the analysis, two regions of interest (ROIs) showed significant alterations in the morphology of GFAP-expressing cells across EMF and drug conditions, specifically in the right hemisphere. This significance was not seen in the left hemisphere. For the general EMF condition, there was a significant increase in the average branching length of GFAP-expressing cells in the right ventromedial hypothalamus when the EMF was applied [$t(32) = -2.52$, $p = 0.017$, $U = 73.0$, $Z = -2.13$, $p = 0.033$]. This can be seen in Figure 1. Furthermore, there was a significant increase in the average branching length of GFAP-expressing cells in the right ventromedial hypothalamus when comparing the low-EMF-intensity conditions [$F(2,30) = 4.55$, $p = 0.019$]. Specifically, there was a significant increase in the average branching length when a $\leq$50 nT EMF was applied, when compared to sham controls [$t(29) = -3.03$, $p = 0.005$]. This can be seen in Figure 2. Additionally, there was a significant main effect for drug condition within the right dentate gyrus of the hippocampus. Specifically, there was a significant decrease in the average surface area of GFAP-expressing cells seen in rats treated with LA when compared to water controls [$t(23) = 2.36$, $p = 0.027$]. This can be seen in Figure 3.

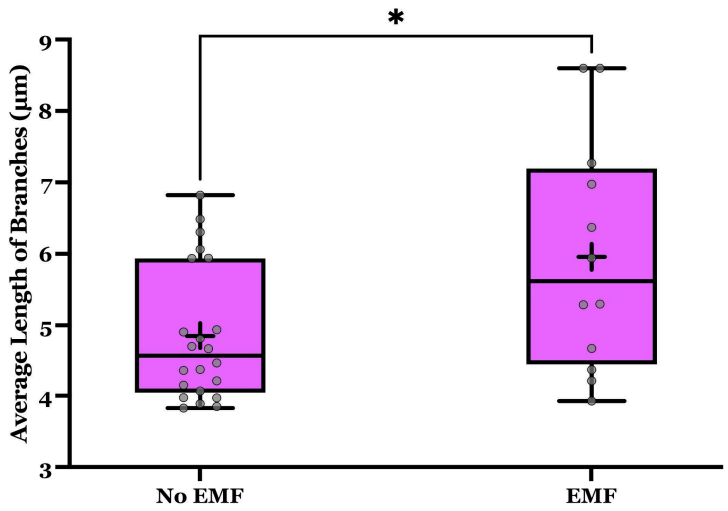


Figure 1. Box and Whisker plot depicting the average length of branches on glial fibrillary acidic protein (GFAP)-expressing cells (µm) in the right ventromedial hypothalamus with respect to the field condition ('no EMF' and 'EMF'). Significant increase in the length of branch for EMF-exposed groups (n = 34), t(32) = −2.52, p = 0.017, U = 73.0, and Z = −2.13, p = 0.033. Circles (°) indicate raw data points, + indicates mean value, and * indicates a significance (p) of <0.05.

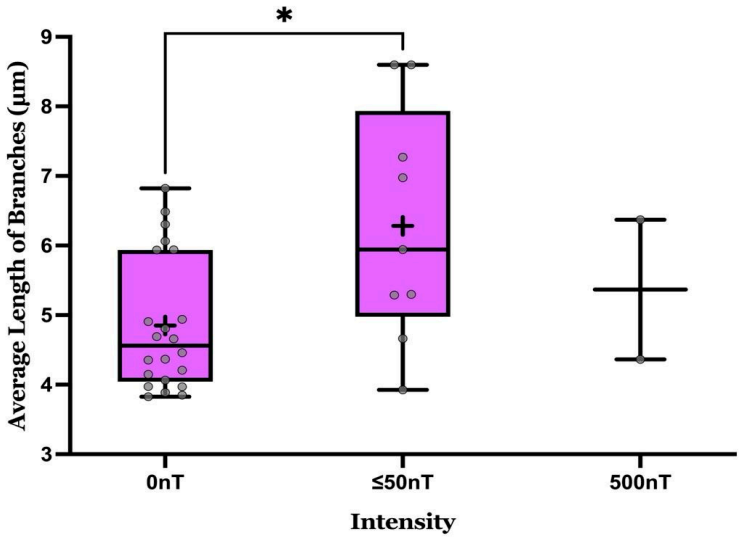


Figure 2. Box and Whisker plot depicting the average length of branches on GFAP-expressing cells (µm) in the right ventromedial hypothalamus across EMF intensities (Int 0 nT, Int ≤50 nT, Int 500 nT) F(2,30) = 4.55, p = 0.019. Significant increase in the average length of branches when rats are exposed to an intensity of ≤50 nT, 0 nT, and ≤50 nT (n = 34); t(29) = −3.03, p = 0.005. Circles (°) represent raw data points, + indicates mean value, and * indicates a significance (p) of <0.05.

3.2. Sex Effects and Drug by EMF Interactions

There were many notable sex effects with the ROIs. Notably, females showed an overall increase in the expression and morphology of GFAP-expressing cells within four of the ROIs when compared to males. These included the left ventromedial hypothalamus [t(31) = −2.11, p = 0.043], the right amygdala [t(36) = −2.38, p = 0.023], the left primary somatosensory cortex [t(35) = −2.03, p = 0.050], and the right entorhinal cortex [t(36) = −2.16, p = 0.037]. A summary of these results can be seen in Table 1. Furthermore, when looking at how each drug condition affected each sex, a significant increase in the average number of branches on GFAP-expressing cells in the right entorhinal cortex in female rats administered either LA [t(10) = −4.01, p = 0.002] or NMA [t(8) = −2.65, p = 0.029] was observed when

compared to males. This increase was not present in the water groups. This can be seen in Figure 4. Additionally, when looking at the interaction between EMF condition and sex, a significant increase in the average number of branches on GFAP-expressing cells is observed in the left CA2 region of the hippocampus [$F(3,31) = 2.99$, $p = 0.046$]. Specifically, it was observed that males exposed to the EMF exhibited significantly more branches on GFAP-expressing cells in the left CA2 region of the hippocampus when compared to their non-exposed counterparts [$t(15) = -2.90$, $p = 0.011$], and to females exposed to the EMF [$t(10) = 2.81$, $p = 0.018$]. This can be seen in Figure 5. Representative GFAP-stained sections from the hippocampus between sex and EMF conditions can be seen in Figure 6. These sections demonstrate pronounced astrocytic presence in the CA2 region under EMF exposure for males. These findings highlight potential sex-dependent effects of the drug conditions and EMF exposure on GFAP expression and cell morphology within the entorhinal cortex and the CA2 region of the hippocampus.

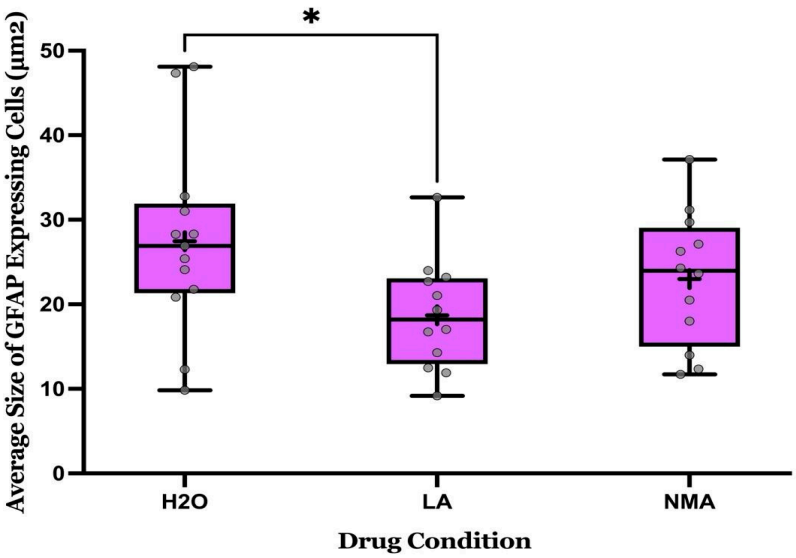


Figure 3. Box and Whisker plot depicting the average surface area of GFAP-expressing cells (μm^2) in the right dentate gyrus of the hippocampus with respect to condition H20, L-Arginine (LA), N-methyl arginine (NMA). Significant decrease in the average surface area of GFAP-expressing cells seen in rats administered LA compared to controls. [$t(23) = 2.36$, $p = 0.027$]. Circles (°) represent raw data points, + indicates mean value, and * indicates a significance (p) of <0.05.

Table 1. Mean, standard deviation (SD), and t-test significance (p) for GFAP expression and cell morphology by sex (male, female) in the left ventromedial hypothalamus, right amygdala, left primary somatosensory cortex, and right entorhinal cortex. Significant increase seen in females when compared to males.

	Male		Female		Significance
	n	**Mean (SD)**	***n***	**Mean (SD)**	
Left Ventromedial Hypothalamus—Total Number of GFAP-Expressing Cells	14	34.428 (28.174)	19	60.315 (38.994)	$p = 0.043$
Right Amygdala—Total Number of GFAP-Expressing Cells	18	39.944 (30.819)	20	66.95 (38.163)	$p = 0.023$

Table 1. *Cont.*

	Male		Female		Significance
	n	**Mean (SD)**	***n***	**Mean (SD)**	
Left Primary Somatosensory Cortex—Total Number of Branches on GFAP-Expressing Cells	17	101.588 (114.709)	20	191.9 (149.916)	$p = 0.050$
Left Primary Somatosensory Cortex—Average Number of Branches on GFAP-Expressing Cells	17	2.556 (1.241)	20	3.616 (1.603)	$p = 0.033$
Right Entorhinal Cortex—Total Area of GFAP-Expressing Cells	18	1028.504 (1336.890)	20	2168.922 (1928.473)	$p = 0.043$
Right Entorhinal Cortex—Total Number of GFAP-Expressing Cells	18	40.388 (36.091)	20	65.2 (34.564)	$p = 0.037$
Right Entorhinal Cortex—Average surface area of GFAP-Expressing Cells	18	13.314 (7.080)	20	19.620 (9.008)	$p = 0.023$
Right Entorhinal Cortex—Total Number of Branches on GFAP-Expressing Cells	18	111.277 (127.048)	20	221 (163.987)	$p = 0.014$
Right Entorhinal Cortex—Average Number of Branches on GFAP-Expressing Cells	18	2.422 (1.381)	20	3.799 (1.715)	$p = 0.005$
Right Entorhinal Cortex—Total Length of Branches on GFAP-Expressing Cells	18	379.401 (422.629)	20	757.676 (546.695)	$p = 0.012$
Right Entorhinal Cortex—Average Length of Branches on GFAP-Expressing Cells	18	3.979 (1.608)	20	4.912 (0.964)	$p = 0.017$

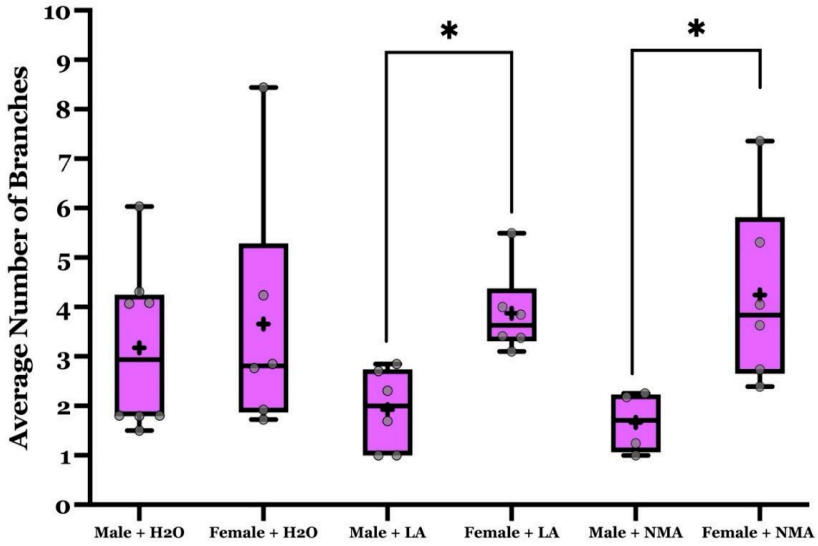


Figure 4. Box and Whisker plot depicting the average number of branches on GFAP-expressing cells in the right entorhinal cortex with respect to drug condition (H_2O, LA, NMA) and sex (male, female). Significant increase in the number of branches on GFAP-expressing cells in females administered LA compared to males administered LA [$t(10) = -4.01$, $p = 0.002$] and in females administered NMA compared to males administered NMA [$t(8) = -2.65$, $p = 0.029$] (n = 36). Circles (°) represent raw data points, + indicates mean value, and * indicates significance (p) <0.05.

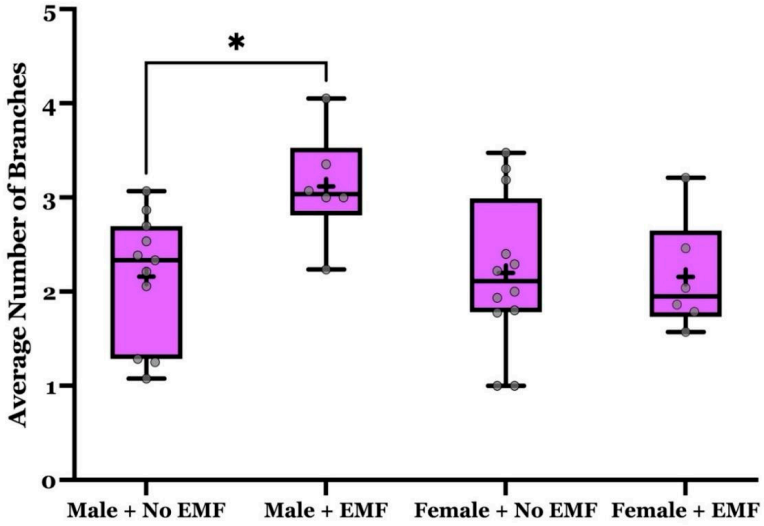


Figure 5. Box and Whisker plot depicting the average number of branches on GFAP-expressing cells in the left CA2 region of the hippocampus with respect to sex (male, female) and field condition (no EMF, with EMF) (n = 34) [$F(3,31) = 2.99$, $p = 0.046$]. Significant increase in the average number of branches is seen in male rats exposed to EMF compared to males not exposed [$t(15) = -2.904$, $p = 0.011$] and to females exposed to EMF [$t(10) = 2.81$, $p = 0.018$]. Circles (°) indicate raw data points, + indicates mean value, and * indicates significance (p) <0.05.

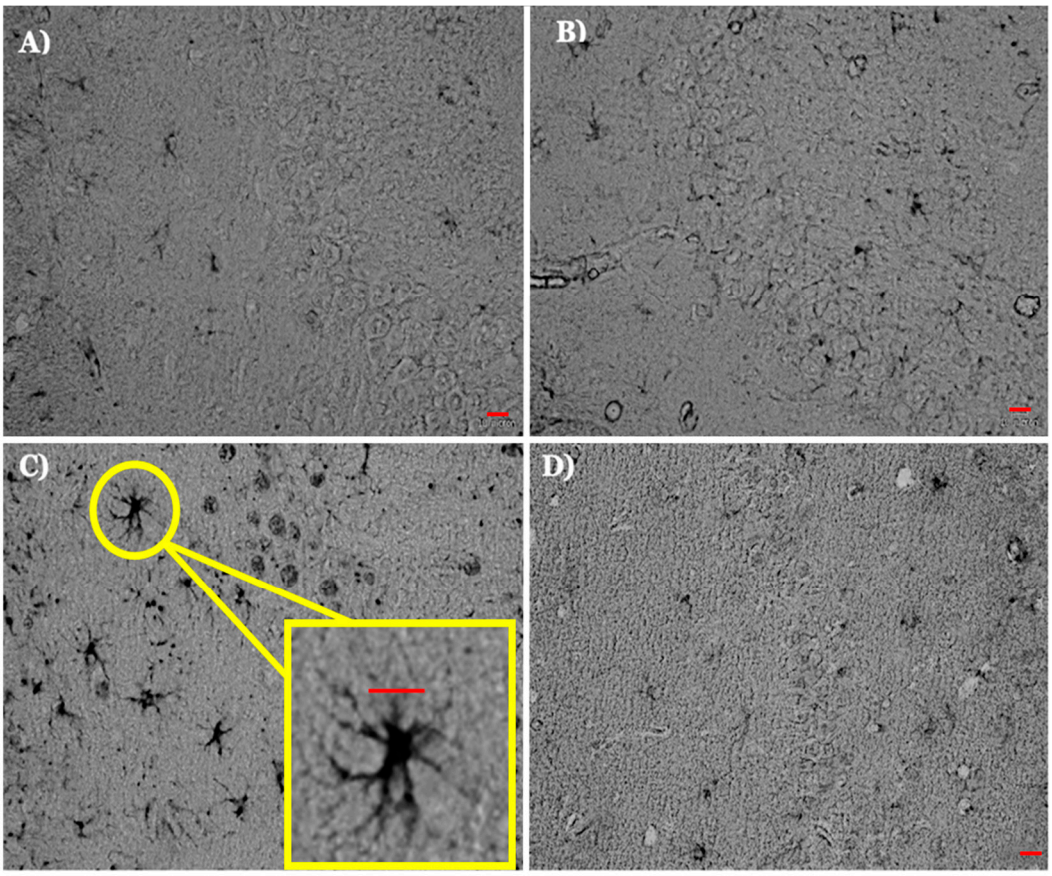


Figure 6. GFAP expression in the left CA2 region of the hippocampus, comparing sex (male, female) and field condition (no EMF, EMF). Dark-black areas represent GFAP-positive astrocytes identified through immunohistochemical staining. Yellow boxes highlight specific astrocytes. (**A**) Male rats with no EMF exposure, (**B**) female rats with no EMF exposure, (**C**) male rats with EMF exposure, and (**D**) female rats with EMF exposure. Scale bars: 10 μm.

4. Discussion

The results of the present study support the previously reported and published data on the interactive effects of EMFs, NO modulation, and sex in the significant changes in the GFAP expression across multiple ROIs observed. Importantly, these changes were observed in rats sacrificed in late adulthood (mean = 568 days, SD = 161), indicating that early-life EMF and nitric oxide exposure induces long-lasting alterations in astrocyte structure and GFAP expression. These results are shown to be preferentially in the right hemisphere and with a slight preference toward female rats in comparison to males. The observed right-hemisphere bias may reflect underlying lateralized differences in astrocyte reactivity, vascular organization, or oxidative stress sensitivity, though the precise mechanisms remain unclear and warrant further investigation. Regardless of sex and drug condition, the morphology of GFAP-expressing cells is significantly changed in the right ventromedial hypothalamus when an EMF is present, particularly if the intensity of the EMF is $\leq$50 nT, whereby the length of the branches on GFAP-expressing cells is increased compared to sham exposed rats. This finding is consistent with previous work suggesting that low-intensity EMFs may influence NOS expression, which can in turn affect astrocytic morphology. However, we did not directly assess NOS activity in this study, and further investigation is required to establish this link. In addition, this finding could provide a possible rationale behind the increase in body weight seen during the previous behavioral study since the ventromedial hypothalamus is known to be associated with satiation. In support of this, it was found that the average length of branching on GFAP-expressing cells was shown to be significantly correlated with the rats' body weight [r = 0.404, p = 0.050, rho = 0.449, p = 0.028], a relationship which was previously discovered by Garcia-Caceres et al. in 2012, where they noted an association between hypothalamic gliosis, weight gain, and obesity [18].

Along with the EMF effects, the administration of the NOS precursor LA was associated with alterations in GFAP-expressing cells, specifically a significant decrease in the average surface area compared to water controls, a finding that is supported by the previous literature, where it was determined that, when the bioavailability of NO is increased using an NO metabolite, such as LA, a reduction in GFAP expression is noted within the CNS [7,16].

In addition to the main effects, there were significant interactions between EMF, drug condition, and the sex of the animal. Supporting the previous literature, female rats displayed higher levels.

GFAP expression occurred across four ROIs, the left ventromedial hypothalamus, the left primary somatosensory cortex, the right amygdala, and the right entorhinal cortex, when compared to males. Furthermore, within the right entorhinal cortex, the increase in the number of branches on GFAP-expressing cells for female rats was observed when compared to males for both the drug conditions, LA and NMA, however no significant difference was shown in the water condition. This finding could point to a sex-specific effect when it comes to the modulation of NO using ingested NOS modulators.

When looking at the interactions between sex and EMF, a significant increase in the number of branches on GFAP-expressing cells in the left CA2 region of the hippocampus was higher in males who were exposed to an EMF compared to male controls and to females who were exposed to an EMF. This significant increase in branching among male rats exposed to the EMF suggests a sex-specific susceptibility to EMF-induced alterations in GFAP expression. This is also shown in the literature when it is stated that females are more susceptible to the effects of EMF exposure compared to males; however, males show higher vulnerability to morphological changes with the CNS [19–21].

In conclusion, the findings of this study highlight the intricate relationship that exists between sex, EMF exposure, hemisphere, and pharmacological interventions in influencing the GFAP expression and cell morphology across various brain regions throughout development. It was observed that, in general, NO modulation and the application of a 7 Hz square-wave EMF had a preferential right-hemispheric effect with four of the ROIs being in the right hemisphere. Additionally, it follows the previous literature in showing that females have a higher expression of the GFAP than males, however males show an increased response to EMF exposure. The results further emphasize the importance and need for considering sex specificity when investigating the effects of environmental influences, which are present during developmental stages. One limitation of this study is the use of archived brain tissue, which may introduce unknown effects related to long-term storage. However, all samples were collected and stored under identical conditions, minimizing the risk of group-specific bias. To build on these findings, future research should incorporate molecular analyses, such as NOS isoform expression, enzymatic activity assays, and downstream signaling markers (e.g., cGMP levels), to better characterize the pathways underlying GFAP modulation in response to EMF exposure and nitric oxide interventions. Expanding this line of investigation is critical for understanding the broader health implications of early-life environmental exposures, particularly as future generations develop in increasingly EMF-saturated environments.

Author Contributions: Conceptualization, S.M.S., N.J.M. and B.T.D.; methodology, S.M.S. and N.J.M.; formal analysis, S.M.S. and B.T.D.; investigation, S.M.S.; resources, N.J.M. and B.T.D.; data curation, S.M.S.; writing—original draft preparation, S.M.S. and B.T.D.; writing—review and editing, S.M.S., N.J.M. and B.T.D. All authors have read and agreed to the published version of the manuscript.

Funding: This research received no external funding.

Institutional Review Board Statement: The paper we submitted did not focus on animal research; it utilized stored tissue. At no point did we handle live animals or require ethics approval. The original study, in which live animals were used, was approved almost 20 years ago by the LU Animal Care Committee. However, since we only used previously collected tissue, no additional ethics approval was required. The Laurentian University Animal Care Committee reviewed and granted permission for this study. Approval code: 980018; approval date: 1 May 2004.

Informed Consent Statement: Not applicable.

Data Availability Statement: Data are available from the corresponding author upon reasonable request.

Acknowledgments: We would like to thank Kassra Ghassemkhani for technical support.

Conflicts of Interest: The authors report no conflicts of interest.

References

1. Jurga, A.M.; Paleczna, M.; Kadluczka, J.; Kuter, K.Z. Beyond the GFAP-astrocyte protein markers in the brain. *Biomolecules* **2021**, *11*, 1361. [CrossRef] [PubMed]
2. Esshili, A.; Manitz, M.P.; Freund, N.; Juckel, G. Induction of inducible nitric oxide synthase expression in activated microglia and astrocytes following pre- and postnatal immune challenge in an animal model of schizophrenia. *Eur. Neuropsychopharmacol.* **2020**, *35*, 100–110. [CrossRef] [PubMed]
3. Rurak, G.M.; Simard, S.; Freitas-Andrade, M.; Lacoste, B.; Charih, F.; van Geel, A.; Stead, J.; Woodside, B.; Green, J.R.; Coppola, G.; et al. Sex differences in developmental patterns of neocortical astroglia: A mouse translatome database. *Cell Rep.* **2022**, *38*, 110310. [CrossRef]
4. Crespo-Castrillo, A.; Arevalo, M.A. Microglial and astrocytic function in physiological and pathological conditions: Estrogenic modulation. *Int. J. Mol. Sci.* **2020**, *21*, 3219. [CrossRef] [PubMed]
5. Kim, K.Y.; Shin, K.Y.; Chang, K.A. GFAP as a Potential Biomarker for Alzheimer's Disease: A Systematic Review and Meta-Analysis. *Cells* **2023**, *12*, 1309. [CrossRef] [PubMed]

6. Zwirner, J.; Lier, J.; Franke, H.; Hammer, N.; Matschke, J.; Trautz, F.; Tse, R.; Ondruschka, B. GFAP positivity in neurons following traumatic brain injuries. *Int. J. Leg. Med.* **2021**, *135*, 2323–2333. [CrossRef] [PubMed]
7. Brahmachari, S.; Fung, Y.K.; Pahan, K. Induction of glial fibrillary acidic protein expression in astrocytes by nitric oxide. *J. Neurosci.* **2006**, *26*, 4930–4939. [CrossRef] [PubMed]
8. Sticozzi, C.; Belmonte, G.; Frosini, M.; Pessina, F. Nitric Oxide/Cyclic GMP-Dependent Calcium Signalling Mediates IL-6- and TNF-α-Induced Expression of Glial Fibrillary Acid Protein. *J. Mol. Neurosci.* **2021**, *71*, 854–866. [CrossRef] [PubMed]
9. Wang, L.; Hagemann, T.L.; Kalwa, H.; Michel, T.; Messing, A.; Feany, M.B. Nitric oxide mediates glial-induced neurodegeneration in Alexander disease. *Nat. Commun.* **2015**, *6*, 8966. [CrossRef] [PubMed]
10. Li, Q.; Zhao, Y.; Guo, H.; Li, Q.; Yan, C.; Li, Y.; He, S.; Wang, N.; Wang, Q. Impaired lipophagy induced-microglial lipid droplets accumulation contributes to the buildup of TREM1 in diabetes-associated cognitive impairment. *Autophagy* **2023**, *19*, 2639–2656. [CrossRef] [PubMed]
11. Béchade, C.; Pascual, O.; Triller, A.; Bessis, A. Nitric oxide regulates astrocyte maturation in the hippocampus: Involvement of NOS2. *Mol. Cell. Neurosci.* **2011**, *46*, 762–769. [CrossRef] [PubMed]
12. Arias, C.; Zepeda, A.; Hernández-Ortega, K.; Leal-Galicia, P.; Lojero, C.; Camacho-Arroyo, I. Sex and estrous cycle-dependent differences in glial fibrillary acidic protein immunoreactivity in the adult rat hippocampus. *Horm. Behav.* **2009**, *55*, 257–263. [CrossRef] [PubMed]
13. Morrison, H.W.; Filosa, J.A. Stroke and the neurovascular unit: Glial cells, sex differences, and hypertension. *Am. J. Physiol.-Cell Physiol.* **2019**, *316*, C325–C339. [CrossRef] [PubMed]
14. Whissell, P.D.; Persinger, M.A. Developmental effects of perinatal exposure to extremely weak 7 Hz magnetic fields and nitric oxide modulation in the Wistar albino rat. *Int. J. Dev. Neurosci.* **2007**, *25*, 433–439. [CrossRef] [PubMed]
15. Sissons, S.M.; Dotta, B.T. Brain structure alterations following neonatal exposure to low-frequency electromagnetic fields: A histological analysis. *Int. J. Dev. Neurosci.* **2024**, *84*, 651–658. [CrossRef] [PubMed]
16. Zhang, X.; Yang, S.-B.; Cheng, L.; Ho, K.; Kim, M.-S. Botanical Mixture Containing Nitric Oxide Metabolite Enhances Neural Plasticity to Improve Cognitive Impairment in a Vascular Dementia Rat Model. *Nutrients* **2023**, *15*, 4381. [CrossRef] [PubMed]
17. Paxinos, G.; Watson, C. *The Rat Brain in Stereotaxic Coordinates*, 7th ed.; Elsevier Academic Press: Amsterdam, The Netherlands, 2014; p. 170.
18. García-Cáceres, C.; Fuente-Martín, E.; Argente, J.; Chowen, J.A. Emerging role of glial cells in the control of body weight. *Mol. Metab.* **2012**, *1*, 37–46. [CrossRef] [PubMed]
19. Ozturk, H.; Saribal, D.; Gelmez, Y.M.; Deniz, G.; Yilmaz, A.; Kirectepe, A.; Ercan, A.M. Extremely low frequency electromagnetic fields exposure during the prenatal and postnatal periods alters pro-inflammatory cytokines levels by gender. *Electromagn. Biol. Med.* **2022**, *41*, 163–173. [CrossRef] [PubMed]
20. Acikgoz, B.; Ersoy, N.; Aksu, I.; Kiray, A.; Bagriyanik, H.A.; Kiray, M. Gender differences in effects of prenatal and postnatal exposure to electromagnetic field and prenatal zinc on behaviour and synaptic proteins in rats. *J. Chem. Neuroanat.* **2022**, *122*, 102092. [CrossRef] [PubMed]
21. Kashani, Z.A.; Pakzad, R.; Fakari, F.R.; Haghparast, M.S.; Abdi, F.; Kiani, Z.; Talebi, A.; Haghgoo, S.M. Electromagnetic fields exposure on fetal and childhood abnormalities: Systematic review and meta-analysis. *Open Med.* **2023**, *18*. [CrossRef]

Disclaimer/Publisher's Note: The statements, opinions and data contained in all publications are solely those of the individual author(s) and contributor(s) and not of MDPI and/or the editor(s). MDPI and/or the editor(s) disclaim responsibility for any injury to people or property resulting from any ideas, methods, instructions or products referred to in the content.